TITLE: Molecular evolution and developmental expression of melanin pathway genes in Lepidoptera

AUTHORS: Muktai Kuwalekar[†], Riddhi Deshmukh[†], Ajay Padvi and Krushnamegh Kunte*

AFFILIATIONS: National Center for Biological Sciences, Tata Institute of Fundamental Research, GKVK Campus, Bellary Road, Bengaluru 560065, India.

[†] These authors contributed equally

CORRESPONDENCE: Krushnamegh Kunte (krushnamegh@ncbs.res.in)

ABSTRACT: Pigmentation is involved in a wide array of biological functions across insect orders, including body patterning, thermoregulation, and immunity. The melanin pathway, in particular, has been characterized in several species. However, molecular evolution of the genes involved in this pathway is poorly characterized, and their roles in pigmentation of early developmental stages are just beginning to be explored in non-model organisms. We traced the molecular evolution of six melanin pathway genes in 53 species of Lepidoptera covering butterflies and moths, and representing over 100 million years of diversification. We compared the rates of synonymous and nonsynonymous substitutions within and between these genes to study signatures of selection at the level of individual sites, genes, and branches of the gene tree. We found that molecular evolution of all six genes was governed by strong purifying selection. Yet, a number of sites showed signs of being under positive selection, including in the highly conserved domain regions of three genes. Further, we traced the expression of these genes across developmental stages, tissues, and sexes in the *Papilio polytes* butterfly using a developmental transcriptome dataset. We observed that the expression patterns of the genes in *P. polytes* largely reflected their known tissue-specific function in other species. The expression of sequentially acting genes in the melanin pathway was correlated. Interestingly, four out of six melanin pathway genes (*ebony*, *pale*, *aaNAT*, and *DDC*) showed a sexually dimorphic pattern of developmental heterochrony; i.e., females showed peak activity much earlier in pupal development compared to that of males. Our evolutionary and developmental analyses suggest that the vast diversity of wing patterning and pigmentation in Lepidoptera may have been aided largely by differential developmental regulation of genes in a highly conserved pathway, in which the sequence evolution of individual genes is highly constrained.

KEYWORDS: melanization, pigmentation, developmental heterochrony, butterfly wing coloration, wing patterns

INTRODUCTION: The evolution of color patterns contributes to the striking diversity of lifeforms. Coloration is a critical adaptation that impacts an organism's intra- and inter-specific communication and interactions. In several cases, emergence of sexual dimorphism and polymorphism is also linked to the evolution and differential expression of pigmentation genes (Wittkopp et al., 2009; Miyazaki et al., 2014; Yassin et al., 2016). Among Lepidoptera, wing coloration and patterning are remarkably diverse, which have shaped several adaptations such as aposematism, crypsis, mimicry, and thermoregulation (True, 2003; Hegna et al., 2013; Olofsson et al., 2013; Kronforst and Papa, 2015; Nadeau, 2016; Deshmukh et al., 2018; van't Hof et al., 2019). In insects, melanins, ommochromes, and pterins are three major biosynthesized pigments deposited in developing wing scales (Wittkopp and Beldade, 2009). Melanin production—being involved in a wide range of physiological processes—is conserved across insect orders. For instance, increased melanization in high-altitude moths aids in thermoregulation, resulting in a trade-off between warning coloration and hindwing melanization (Hegna et al., 2013). Melanization is also associated with immunity, wound healing, and protection from both ultraviolet light and parasitoids (Yassine et al., 2012; Bilandžija et al., 2017). Melanin and related pigments—such as DOPA-melanin, dopamine-melanin, NBAD sclerotin, and NADA sclerotin—contribute to the production of black, brown, and yellow coloration (Wright, 1987, Koch et al., 2000; Zhang et al., 2017). The availability of genetic manipulation techniques in non-model systems has allowed elucidation of the role of melanin pathway genes in color adaptations (Zhang and Reed, 2017; Zhang et al., 2017a; Matsuoka and Monteiro, 2018). While the developmental mechanisms underlying pigmentation and patterning are being extensively studied, the evolutionary trajectories of these pigmentation genes remain poorly explored.

We chose six melanin pathway genes—*tan*, *black*, *ebony*, *pale* (*tyrosine hydroxylase*), *arylalkylamine N-acetyltransferase 1* (*aaNAT*) and *DOPA decarboxylase* (*DDC*)—whose developmental function in Lepidoptera coloration is well characterized (Zhang et al., 2017a; Matsuoka and Monteiro, 2018). The functions and phenotypic effects of these genes are summarized in Fig. 1 and Table S1. Melanin synthesis occurs by a branched pathway with tyrosine and uracil as precursors, and different end products (Wright, 1987; Matsuoka and Monteiro, 2018). These precursors are shunted into the melanin pathway by *pale* and *DDC* (Zhang et al., 2017a). *black, ebony,* and *tan* are involved in the synthesis of N-β-alanyl dopamine (NBAD), which is responsible for yellow coloration, while *aaNAT* facilitates the formation of colorless cuticles essential for wing pigmentation (Fig. 1, Table S1). These genes are thus crucial for melanin production and its deposition on Lepidoptera wings. The pigments observed in adults start appearing on the wings and body tissues during late pupal stages, and black melanin is usually the last one to be deposited (Koch et al., 1998; Wittkopp and Beldade, 2009; Matsuoka and Monteiro, 2018). In this study, we trace the molecular evolution of these six genes in 53 species across nine superfamilies of Lepidoptera (total over 100 million years of divergence), and additionally characterize their expression patterns across various developmental stages and tissues of *Papilio polytes* to address the following questions: (a) what selection pressures have shaped the evolution of these genes in the Lepidoptera?, (b) Do these genes show differential activity in sexually

dimorphic species?, and (c) Do they play similar roles in larval pigmentation and adult wing patterning and pigmentation?

MATERIALS AND METHODS:

Gene sequences and multiple sequence alignment: We downloaded whole genome sequences of 53 species of Lepidoptera from GenBank (http://www.ncbi.nlm.nih.gov), LepBase (http://www.lepbase.org), and GigaDB (http://www.re3data.org), which best represented different families. We selected six genes which are central to pigmentation and patterning pathways namely *tan*, *black*, *ebony*, *pale* (*tyrosine hydroxylase*), *aaNAT* (*Arylalkylamine N-acetyltransferase 1*) and *DDC* (*dopa decarboxylase*) (Wright, 1987; Zhang et al., 2017a; Matsuoka and Monteiro, 2018). We performed exon-wise NCBI local tBLASTn to locate these genes within genomes of the selected species (Table S2). For all the genes, we chose the longest isoform for performing tBLASTn as it incorporates maximum sequence information for the given gene. Using these gene coordinates, we extracted respective genes from the genome using an in-house python script. The downloaded genome sequences showed no evidence of duplication for any of the six melanin pathway genes. Several genome files (such as those of *Bicyclus anynana, Papilio polytes, Papilio xuthus* and *Bombyx mori*) had annotated two copies of *aaNAT* and *black*, but they shared low similarity scores (~40%) and were therefore not considered as duplicates in our analysis. We performed multiple sequence alignment of each gene with MEGA X muscle aligner with codon alignment option (Kumar et al., 2018). We included homologous gene sequences from Diptera as outgroups for respective genes.

Gene tree construction and phylogenetic analysis: We constructed a species-level phylogeny with two mitochondrial (*cytochrome c oxidase I*, *acetyl-CoA acetyltransferase*) and eleven nuclear genes (*elongation factor 1 – alpha*, *wingless*, *ribosomal Protein S5*, *ribosomal protein S2*, *isocitrate dehydrogenase*, *DOPA decarboxylase*, *glyceraldehyde-3-phosphate dehydrogenase*, *malate dehydrogenase*, *catalase*, *CAD*, *ribosomal protein S27a / hairy cell leukemia*) that are used commonly in phylogenetic reconstruction (Wahlberg and Wheat, 2008). We performed multiple sequence alignment on these thirteen markers using the codon aligner PRANK v150803 (Löytynoja and Goldman, 2005). For construction of species and gene trees, we calculated the best partition scheme and corresponding sequence evolution model using Partition Finder 2.1.1 (Lanfear et al., 2016). We chose greedy algorithm and Mr. Bayes model of evolution. We selected Bayesian information criterion to compare and choose from the best-fit models. We used a split frequency below 0.01 to assess stationarity and to set the burn-in in Mr. Bayes and then built a consensus tree using the remaining trees (Ronquist et al., 2012).

Determination of synonymous (dS) and nonsynonymous (dN) substitution rates: To calculate site-wise synonymous and nonsynonymous substitution rates of each gene, we used their respective MUSCLE alignments and the Fixed Effect Likelihood (FEL) method with a maximum-likelihood (ML) approach (Kosakovsky Pond and Frost, 2005). We plotted and compared codon-wise dN, dS, and dN/dS values for each gene (Fig. 2) and performed a Kruskal-Wallis test followed by Dunn's test with Bonferroni correction in R (Derek et al., 2020) We also identified sites that

have been subjected to pervasive diversification (dN/dS > 1) or purifying selection (dN/dS < 1) within every gene using FEL. We calculated global omega (R value, which represents dN/dS for the entire sequence) for respective alignments using AnalyzeCodonData function of HyPhy 2.3.14 (Pond et al., 2005; Kosakovsky Pond et al., 2020) (Table 1). To identify conserved domains in the given proteins, we used the Conserved Domain Database (CDD) and the CD-Search Tool (Marchler-Bauer et al., 2012).We separately performed FEL analysis and estimated global omega for these domains to compare gene-wide and domain-wide signatures of selection (Fig. 2 and Table 1).

Branch level, gene-wide and site-wise assessment of molecular evolution: We used aBSREL (adaptive Branch-Site Random Effects Likelihood) method to test for positive selection along each gene tree (Kosakovsky Pond et al., 2011; Smith et al., 2015). We used BUSTED to investigate if any of the six genes have experienced positive selection in at least one site. We carried out MEME (Mixed Effects Model of Evolution) which takes maximum-likelihood approach to test whether individual sites have been subjected to episodic positive or diversifying selection (dN/dS > 1). We performed FEL, MEME, BUSTED and aBSREL on the Datamonkey Adaptive Evolution Server (Weaver et al., 2018), processing the data using in-house scripts.

Sample collection, RNA extraction, and transcriptome sequencing for quantification of expression: We bred greenhouse populations of *Papilio polytes* from mated wild-caught females. We maintained larvae at 28±4°C on lemon (*Citrus sp.*) and curry plants (*Murraya koenigii*) and adults on Birds Choice™ butterfly nectar. We preserved *Papilio polytes* at different stages of metamorphosis in TRIzol™. We collected eggs at 2, 10 and 24 hours, and at 3 days after oviposition, and pooled five eggs for each sample to get sufficient amount of RNA. We sampled larvae at 1st, 3rd and 5th instars. For RNA extraction, we used gutted bodies of 1st and 3rd instar larvae and dissected wing discs from 5th instar larvae and pre-pupae to get three tissue types—forewings, hindwings and gutted body. We collected pupae at 3, 6, and 9 days after pupation, and dissected them to separate the forewings, hindwings, abdomen, thorax, and head. Several pigmentation pathway genes participate in transport and phototransduction in insect eyes (True et al., 2005, Zeigler, 2012). To account for altered sensitivity and visual perception due to the mating status of the butterflies, if any, we collected unmated and mated adults separately and further dissected them to separate abdomen, head, eyes, and thorax. We used pure-breeding mimetic lines for this study. We sampled eggs, 1st and 3rd instar larvae in triplicates, 5th instar larvae, pre-pupae and pupae in duplicates for males and females each, and adults in quadruplets for each sex.

We extracted RNA from preserved tissues using the chloroform-isopropanol-based extraction method. We prepared libraries using TruSeq® RNA Sample Preparation Kit v2 and used Qubit fluorometric quantification. We also used Bioanalyzer to check library profiles. For transcriptome sequencing we used 2x100 PE runs on Illumina HiSeq 2500 and obtained ~20 million reads for each sample. We performed quality check on these reads using FASTQ, trimmed them using Trimmomatic and aligned them to *P. polytes* reference genome (Nishikawa et al., 2015) using STAR aligner for eggs, larvae and pupae and HISAT2 aligner for adults. We used HTSeq

for obtaining raw counts and edgeR pipeline for analyzing and plotting gene expression for all the genes.

RESULTS:

Melanin pathway genes are single-copy conserved genes under strong purifying selection in Lepidoptera. We reconstructed gene trees for each of the six genes (Fig. S1). Each gene tree was well-supported and it essentially mirrored the species tree in terms of species relationships and divergence, except *aaNAT,* which had poor resolution with a high degree of polytomy. Absence of long branches and broad similarity with the species tree suggest that these genes have evolved with species divergence and do not seem to have undergone rapid evolution that would be incongruent with the species tree in any lineage.

We plotted dN/dS values for each site in each gene (Fig. 2). The molecular evolution of these genes was characterized by predominantly synonymous substitutions, suggesting constrained evolution (dN/dS values for most sites were well below 1, with mean dN/dS value for each gene ranging from 0.04-0.10). Rates for gene-wide synonymous substitutions were similar, but nonsynonymous rates were significantly different between three groups of genes: *black* and *DDC*; *ebony*, *tan* and *aaNAT;* and *pale* (Dunn's test, $p<0.001$) (Table S3). Overall, >80% sites showed signatures of pervasive purifying selection ($p<0.05$), but no sites showed signatures of pervasive diversifying selection in any melanin pathway genes (Table 1).

All the genes had a single functional domain except for *ebony*, which contained two (Fig. 2). R values were consistently lower for functional domains compared to the gene-wide values (Table 1). This slight difference between domain-wide and gene-wide R values suggests that these genes are nearly as conserved as their functional domains. In some cases, this may be a result of the domain spanning a large portion of the gene. We observed that the nonsynonymous substitution rate was lowest in *pale*, followed by *black* and *DDC* (Fig. 2, $p<0.05$). Since *DDC*, *black,* and *pale* are essential for the synthesis of dopamine—a precursor for multiple pathways including neuromodulation, immune functions, and the circadian cycle (Basu and Dasgupta, 2000; Shang et al., 2011; Allen et al., 2011)—the low dN/dS as well as global R values were expected for these genes. On the other hand, *tan*, *aaNAT* and *ebony* yielded high R values, indicating that they may have evolved under relatively relaxed selection (Fig. 2, Table 1).

Melanin pathway genes show signs of episodic positive selection. In spite of the overall constrained molecular evolution of the six genes, six sites showed signatures of episodic diversifying selection ($p<0.05$) in *aaNAT*, *ebony* and *tan*, including some in the otherwise highly conserved domain regions (Fig. 2, Table 1). Interestingly, although *pale* generally shows very constrained molecular evolution similar to *DDC* and *black*, it also had two sites under episodic positive selection. While BUSTED could not detect gene-wide episodic diversifying selection in *DDC* and *tan*, aBSREL found evidence for it in all the genes except *DDC*.

Melanin pathway genes show stage-specific, often sexually dimorphic expression. We traced the expression of the six genes across different developmental stages, tissues, and sexes in the developmental transcriptome of *Papilio polytes*. *aaNAT, DDC,* and *pale* showed similar patterns

of expression across stages and tissues, as did *black* and *ebony* (Fig. 3). Since *pale, DDC,* and *aaNAT* convert tyrosine to N-acetyl-dopamine in successive reactions with no intermediates (Fig. 1), we expected similar activity patterns of these genes. *aaNAT, DDC* and *pale* showed similar activity across stages with a peak in the pre-pupal stage (Fig. 3), but *pale* additionally showed sexually dimorphic expression at this stage. *DDC* and *pale* expression in most tissues and stages suggests a more general function than melanization-specific activity. Although *ebony* combines the products of *black* and *DDC* to produce NBAD (Fig. 1), its expression pattern was similar to that of *black,* not *DDC.* This suggests that *ebony* activity is more dependent on *black* than on *DDC*. This needs to be experimentally verified. In addition, *ebony* expression also showed sexual dimorphism in pre-pupal stage, while *black* did not.

Unlike any of the other genes, *tan* had a remarkably distinct pattern of expression across development. It showed little to no expression in wings but it was expressed in 1st and 3rd instar larvae, suggesting possible involvement in larval melanization. Expression of *tan*, *black,* and *ebony* in adult eyes and head may have resulted from their role in photo-transduction. For example, *tan* is involved in metabolism of neurotransmitters in photoreceptors, while *ebony* and *black* play a role in signal transduction in the optic lobe (True et al., 2005, Zeigler, 2012). Because of this, we further tested whether mated and unmated females show differential expression since female visual systems may switch from mate choice to host plant search after mating. However, expression of these genes was similar in unmated and mated females as well as in males.

Finally, four melanin pathway genes (*ebony*, *pale*, *aaNAT*, and *DDC*) showed higher expression during larval and early pupal development (pre-pupa and 3-day pupa) in females, but higher expression later in 9-day pupae in males (Fig. 3, Fig. S2). This pattern suggests sex-specific developmental heterochrony.

DISCUSSION: The melanin pathway is complex and versatile, with products of intermediately placed genes feeding into cross-pathways, performing diverse biological functions (Fig. 1). The feasibility of genetic manipulation in non-model organisms has made it possible to understand the extent of role played by each gene in pigment production in a wide range of organisms (Mazo-Vargas et al., 2017; Zhang et al., 2017a, 2017b; Connahs et al., 2019). We supplement this understanding by studying the molecular evolution of six genes (*tan*, *black*, *ebony*, *pale*, *aaNAT* and *DDC*) in the melanin pathway that have prominent roles in color production in butterflies and moths (Koch, 1995; Koch et al., 2000a, 2000b; Futahashi and Fujiwara, 2005; Futahashi et al., 2010; Zhang et al., 2017a; Matsuoka and Monteiro, 2018). With each gene governing a generalized or specialized step, the pathway experiences varied constraints at different levels. We estimated synonymous and nonsynonymous substitution rates for each gene using sequence data, and tested for signatures of selection. Our study shows that these six genes are highly conserved, despite 100 million years of evolutionary divergence across the sampled Lepidopteran superfamilies (Misof et al., 2014). However, the degree of conservation varies across genes, and most of them even show some signatures of episodic and positive selection.

Our selection analysis revealed that all the melanin pathway genes studied here show signatures of strong purifying selection. The dearth of nonsynonymous substitutions across these genes indicates a lack of pervasive diversifying selection at a sequence level, although the developmental regulation of these genes produces dissimilar color patterns across species (Wittkopp et al., 2009; Miyazaki et al., 2014; Yassin et al., 2016). While testing for episodic diversifying selection at the levels of individuals sites, branches and genes, *aaNAT*, *black*, *ebony*, *pale* and *tan*, but not *DDC*, showed evidence of diversifying selection. Similarly, we did not find any site-level evidence for diversifying selection in *black*. These differential signatures of selection across the genes are consistent with their estimated nonsynonymous substitutions, which shows that *black* and *DDC* have followed more constrained evolutionary trajectories compared to the other four genes. Our study does not offer insights into the functional roles of these sites under diversifying selection. However, it does point out potential developmental genetic targets for future manipulative experiments. The functional roles of these sites may also become clear using protein structural analysis.

We obtained a few contradictory results in our selection analysis with the three methods used. For example, gene-level analysis using BUSTED inferred the presence of episodic diversifying selection in *black*, but MEME could not detect individual sites under selection. This may be because BUSTED is capable of combining information from weak sites to infer presence of selection at the whole-gene level, unlike MEME, which detects individual sites and might therefore underestimate sites under selection at the gene level. Similarly, we performed branch-level tests of diversifying selection with aBSREL, whose exploratory module is less likely to detect selection compared to targeted testing (Kosakovsky Pond et al., 2011; Smith et al., 2015). This may have resulted in *aaNAT* not showing branch-level selection despite showing site-level and gene-level diversifying selection using other methods.

We explored the spatio-temporal activity of melanin pathway genes in *P. polytes* using a developmental transcriptome dataset. The first four instars of *P. polytes* larvae mimic bird droppings with black, brown, and white coloration on their bodies. We expected to detect activity of melanin pathway genes in the eggs and 1st and 3rd larval instars. However, we did not find substantial larval expression of any of the six genes (except *tan*) even though knockout phenotypes in previous studies have reported a lack of larval pigmentation (Zhang et al., 2017a; Matsuoka and Monteiro, 2018). It is possible that the low expression that we detected suffices in triggering melanization, or we may have missed the transient stage where melanin pathway genes are upregulated in early development. Exploring the expression patterns of other genes in the pathway, such as *laccase2* and *yellow*, may help corroborate either hypothesis. The expression patterns of genes also showed signs of sex-specific developmental heterochrony in melanin production, with expression during pupal development peaking early in females and late in males. While this could be an artefact of sampling, in some cases (especially between male and female pre-pupae and 9-day old pupae), the difference is quite stark. It is possible that males and females differentially invest in melanin production and immunity (or other functions that require melanin pathway intermediates), which would also explain the heterochrony we observed. However, this needs

277 further investigation. With the additional complexity of mimicry in this species, and the use of
278 only mimetic females in this study, the effect of mimicry-related wing-pattern reorganization on
279 melanin pathway genes remains to be explored, and could perhaps be linked to the developmental
280 heterochrony.
281 Melanin pathway genes such as *tan, ebony* and *yellow* are involved in the evolution of color
282 pattern-related sexual dimorphism and polymorphism (Wittkopp et al., 2009; Miyazaki et al.,
283 2014; Yassin et al., 2016), suggesting that these genes have the potential to evolve novel functions
284 despite evolutionarily constrained sequences. Many butterflies and moths exhibit sexual
285 dimorphism and/or female polymorphism, so they are good systems to study signatures of
286 selection in such clades. This would also require information regarding functional allelic variation
287 and duplicated copies of these genes, which we did not encounter in the species that we studied.
288 Alternatively, examining the regulatory regions of these genes and tracing the molecular evolution
289 of upstream regulators might help detect such signals. We have excluded *yellow* gene family from
290 our study even though substantial work has been done on this in flies and butterflies (Arnoult et
291 al., 2013; Miyazaki et al., 2014; Camino et al., 2015; Zhang et al., 2017a; Matsuoka and Monteiro,
292 2018). We were unable to identify sequences of this gene family from the downloaded genome
293 sequences with sufficient confidence due to issues with sequence similarity scores. However, the
294 evolution of this gene family has been explored previously (Ferguson et al., 2011).
295 Our work demonstrates that molecular sequences of the six melanin pathway genes are
296 highly conserved across the vastly diverse Lepidoptera, yet they show some signatures of positive
297 selection. The pattern of conservation and divergence of these genes may be a direct outcome of
298 their functions. We also explored the developmental expression of these genes across tissues and
299 sexes, which recapitulates what we observe in adult stages, but does not provide insights into larval
300 pigmentation. Our work provides a framework in which broad comparisons can be made across
301 genes and species to understand the genetics and evo-devo of complex pathways that produce the
302 remarkable color patterns displayed by insects.
303
304 **ACKNOWLEDGEMENTS:** We thank Atharva Khotpal, Bhavanarayeni R., Sai Guha and
305 Sarvesh Menon for assistance in downloading and analyzing genome sequences; Saurav Baral and
306 Vinod Shankar for help with molecular evolution analysis; Sergei L. Kosakovsky Pond for
307 valuable inputs on HyPhy; NCBS Sequencing Facility for transcriptome sequencing; and NCBS
308 Greenhouse Facility for butterfly breeding facilities.
309 **Funding:** This work was partially funded by an NCBS Research Grant to KK, support of the
310 Department of Atomic Energy, Government of India, under project nos. 12-R&D-TFR-5.04-0800
311 and 12-R&D-TFR-5.04-0900, and a CSIR Shyama Prasad Mukherjee Fellowship to RD.
312 **AUTHORS CONTRIBUTION:** RD and KK designed the study; MK and AP downloaded
313 sequence data and performed molecular evolution analysis; RD performed developmental
314 transcriptome sequencing and analysis; MK and RD prepared figures and wrote the manuscript;
315 KK conceived and directed the project.
316 **Conflict of interest:** The authors declare that they have no competing interests.

REFERENCES

Allen, J. M., Van Kummer, B. H., and Cohen, R. W. (2011). Dopamine as an anorectic neuromodulator in the cockroach *Rhyparobia maderae*. *J. Exp. Biol.* 214, 3843–3849. doi:10.1242/jeb.062430.

Arnoult, L., Su, K. F. Y., Manoel, D., Minervino, C., Magriña, J., Gompel, N., et al. (2013). Emergence and diversification of fly pigmentation through evolution of a gene regulatory module. *Science* 339, 1423–6. doi:10.1126/science.1233749.

Basu, S., and Dasgupta, P. S. (2000). Dopamine, a neurotransmitter, influences the immune system. *J. Neuroimmunol.* 102, 113–124. doi:10.1016/S0165-5728(99)00176-9.

Bilandžija, H., Laslo, M., Porter, M. L., and Fong, D. W. (2017). Melanization in response to wounding is ancestral in arthropods and conserved in albino cave species. *Sci. Rep.* 7, 17148. doi:10.1038/s41598-017-17471-2.

Camino, E. M., Butts, J. C., Ordway, A., Vellky, J. E., Rebeiz, M., and Williams, T. M. (2015). The evolutionary origination and diversification of a dimorphic gene regulatory network through parallel innovations in *cis* and *trans*. *PLOS Genet.* 11, e1005136. doi:10.1371/journal.pgen.1005136.

Connahs, H., Tlili, S., van Creij, J., Loo, T. Y. J., Banerjee, T. Das, Saunders, T. E., et al. (2019). Activation of butterfly eyespots by Distal-less is consistent with a reaction-diffusion process. *Development* 146, dev169367. doi:10.1242/dev.169367.

Derek;, O., Powell, W., and Dinno, A. (2020). FSA: Fisheries Stock Analysis. Available at: https://github.com/droglenc/FSA.

Deshmukh, R., Baral, S., Gandhimathi, A., Kuwalekar, M., and Kunte, K. (2018). Mimicry in butterflies: co-option and a bag of magnificent developmental genetic tricks. *WIREs Dev. Biol.* 7, e291. doi:https://doi.org/10.1002/wdev.291.

Ferguson, L. C., Green, J., Surridge, A., and Jiggins, C. D. (2011). Evolution of the insect *yellow* gene family. *Mol. Biol. Evol.* 28, 257–272. doi:10.1093/molbev/msq192.

Futahashi, R., Banno, Y., and Fujiwara, H. (2010). Caterpillar color patterns are determined by a two-phase melanin gene prepatterning process: new evidence from *tan* and *laccase2*. *Evol. Dev.* 12, 157–167. doi:10.1111/j.1525-142X.2010.00401.x.

Futahashi, R., and Fujiwara, H. (2005). Melanin-synthesis enzymes coregulate stage-specific larval cuticular markings in the swallowtail butterfly, *Papilio xuthus*. *Dev. Genes Evol.* 215, 519–529.

Hegna, R. H., Nokelainen, O., Hegna, J. R., and Mappes, J. (2013). To quiver or to shiver: increased melanization benefits thermoregulation, but reduces warning signal efficacy in the wood tiger moth. *Proc. R. Soc. B* 280, 20122812. doi:10.1098/rspb.2012.2812.

Koch, B. P., Behnecke, B., Weigmann-Lenz, M., and Ffrench-Constant, R. H. (2000a). Insect pigmentation: activities of beta-alanyldopamine synthase in wing color patterns of wild-type and melanic mutant swallowtail butterfly Papilio glaucus. *Pigment cell Res.* 13 Suppl 8, 54–8. Available at: http://www.ncbi.nlm.nih.gov/pubmed/11041358.

Koch, B. P., Keys, D. N., Rocheleau, T., Aronstein, K., Blackburn, M., Carroll, S. B., et al. (1998). Regulation of *dopa decarboxylase* expression during colour pattern formation in wild-type and melanic tiger swallowtail butterflies. *Development* 125, 2303–2313.

Koch, P. B. (1995). Colour pattern specific melanin synthesis is controlled by ecdysteroids via dopa decarboxylase in wings of *Precis coenia* (Lepidoptera: Nymphalidae). *Eur. J. Entomol.* 92, 161–167.

363 Koch, P. B., Behnecke, B., and Ffrench-Constant, R. H. (2000b). The molecular basis of
364 melanism and mimicry in a swallowtail butterfly. *Curr. Biol.* 10, 591–594.
365 Kosakovsky Pond, S. L., and Frost, S. D. W. (2005). Not so different after all: a comparison of
366 methods for detecting amino acid sites under selection. *Mol. Biol. Evol.* 22, 1208–22.
367 doi:10.1093/molbev/msi105.
368 Kosakovsky Pond, S. L., Murrell, B., Fourment, M., Frost, S. D. W., Delport, W., and Scheffler,
369 K. (2011). A random effects branch-site model for detecting episodic diversifying selection.
370 *Mol. Biol. Evol.* 28, 3033–3043. doi:10.1093/molbev/msr125.
371 Kosakovsky Pond, S. L., Poon, A. F. Y., Velazquez, R., Weaver, S., Hepler, N. L., Murrell, B.,
372 et al. (2020). HyPhy 2.5—A customizable platform for evolutionary hypothesis testing
373 using phylogenies. *Mol. Biol. Evol.* 37, 295–299. doi:10.1093/molbev/msz197.
374 Kronforst, M. R., and Papa, R. (2015). The functional basis of wing patterning in *Heliconius*
375 butterflies: the molecules behind mimicry. *Genetics* 200, 1–19.
376 doi:10.1534/genetics.114.172387.
377 Kumar, S., Stecher, G., Li, M., Knyaz, C., and Tamura, K. (2018). MEGA X: Molecular
378 evolutionary genetics analysis across computing platforms. *Mol. Biol. Evol.* 35, 1547–1549.
379 doi:10.1093/molbev/msy096.
380 Lanfear, R., Frandsen, P. B., Wright, A. M., Senfeld, T., and Calcott, B. (2016). PartitionFinder
381 2: new methods for selecting partitioned models of evolution for molecular and
382 morphological phylogenetic analyses. *Mol. Biol. Evol.* 34, 772–773.
383 doi:10.1093/molbev/msw260.
384 Löytynoja, A., and Goldman, N. (2005). An algorithm for progressive multiple alignment of
385 sequences with insertions. *Proc. Natl. Acad. Sci. USA* 102, 10557–62.
386 doi:10.1073/pnas.0409137102.
387 Marchler-Bauer, A., Zheng, C., Chitsaz, F., Derbyshire, M. K., Geer, L. Y., Geer, R. C., et al.
388 (2012). CDD: conserved domains and protein three-dimensional structure. *Nucleic Acids*
389 *Res.* 41, D348–D352. doi:10.1093/nar/gks1243.
390 Matsuoka, Y., and Monteiro, A. (2018). Melanin pathway genes regulate color and morphology
391 of butterfly wing scales. *Cell Rep.* 24, 56–65. doi:10.1016/j.celrep.2018.05.092.
392 Mazo-Vargas, A., Concha, C., Livraghi, L., Massardo, D., Wallbank, R. W. R., Zhang, L., et al.
393 (2017). Macroevolutionary shifts of *WntA* function potentiate butterfly wing-pattern
394 diversity. *Proc. Natl. Acad. Sci.* 114, 10701–10706. doi:10.1073/pnas.1708149114.
395 Misof, B., Liu, S., Meusemann, K., Peters, R. S., Donath, A., Mayer, C., et al. (2014).
396 Phylogenomics resolves the timing and pattern of insect evolution. *Science* 346, 763–767.
397 Miyazaki, S., Okada, Y., Miyakawa, H., Tokuda, G., Cornette, R., Koshikawa, S., et al. (2014).
398 Sexually dimorphic body color is regulated by sex-specific expression of *yellow* gene in
399 ponerine ant, *Diacamma* sp. *PLoS One* 9, e92875. doi:10.1371/journal.pone.0092875.
400 Nadeau, N. J. (2016). Genes controlling mimetic colour pattern variation in butterflies. *Curr.*
401 *Opin. Insect Sci.* 17, 24–31. doi:http://dx.doi.org/10.1016/j.cois.2016.05.013.
402 Nishikawa, H., Iijima, T., Kajitani, R., Yamaguchi, J., Ando, T., Suzuki, Y., et al. (2015). A
403 genetic mechanism for female-limited Batesian mimicry in *Papilio* butterfly. *Nat. Genet.*
404 47, 1–7. doi:10.1038/ng.3241.
405 Olofsson, M., Løvlie, H., Tibblin, J., Jakobsson, S., and Wiklund, C. (2013). Eyespot display in
406 the peacock butterfly triggers antipredator behaviors in naïve adult fowl. *Behav. Ecol.* 24,
407 305–310. doi:10.1093/beheco/ars167.
408 Pond, S. L. K., Frost, S. D. W., and Muse, S. V (2005). HyPhy: hypothesis testing using

409 phylogenies. *Bioinformatics* 21, 676–9. doi:10.1093/bioinformatics/bti079.
410 Ronquist, F., Teslenko, M., van der Mark, P., Ayres, D. L., Darling, A., Höhna, S., et al. (2012).
411 MrBayes 3.2: efficient Bayesian phylogenetic inference and model choice across a large
412 model space. *Syst. Biol.* 61, 539–42. doi:10.1093/sysbio/sys029.
413 Shang, Y., Haynes, P., Pírez, N., Harrington, K. I., Guo, F., Pollack, J., et al. (2011). Imaging
414 analysis of clock neurons reveals light buffers the wake-promoting effect of dopamine. *Nat.*
415 *Neurosci.* 14, 889–895. doi:10.1038/nn.2860.
416 Smith, M. D., Wertheim, J. O., Weaver, S., Murrell, B., Scheffler, K., and Kosakovsky Pond, S.
417 L. (2015). Less is more: an adaptive branch-site random effects model for efficient
418 detection of episodic diversifying selection. *Mol. Biol. Evol.* 32, 1342–1353.
419 doi:10.1093/molbev/msv022.
420 True, J. R. (2003). Insect melanism: the molecules matter. *Trends Ecol. Evol.* 18, 640–647.
421 doi:10.1016/j.tree.2003.09.00.
422 van't Hof, A. E., Reynolds, L. A., Yung, C. J., Cook, L. M., and Saccheri, I. J. (2019). Genetic
423 convergence of industrial melanism in three geometrid moths. *Biol. Lett.* 15, 20190582.
424 doi:10.1098/rsbl.2019.0582.
425 Vavricka, C. J., Christensen, B. M., and Li, J. (2010). Melanization in living organisms: a
426 perspective of species evolution. *Protein Cell* 1, 830–41. doi:10.1007/s13238-010-0109-8.
427 Wahlberg, N., and Wheat, C. W. (2008). Genomic outposts serve the phylogenomic pioneers:
428 designing novel nuclear markers for genomic DNA extractions of Lepidoptera. *Syst. Biol.*
429 57, 231–242. doi:10.1080/10635150802033006.
430 Weaver, S., Shank, S. D., Spielman, S. J., Li, M., Muse, S. V, and Kosakovsky Pond, S. L.
431 (2018). Datamonkey 2.0: A modern web application for characterizing selective and other
432 evolutionary processes. *Mol. Biol. Evol.* 35, 773–777. doi:10.1093/molbev/msx335.
433 Wittkopp, P. J., and Beldade, P. (2009). Development and evolution of insect pigmentation:
434 Genetic mechanisms and the potential consequences of pleiotropy. *Semin. Cell Dev. Biol.*
435 20, 65–71. doi:10.1016/j.semcdb.2008.10.002.
436 Wittkopp, P. J., Stewart, E. E., Arnold, L. L., Neidert, A. H., Haerum, B. K., Thompson, E. M.,
437 et al. (2009). Intraspecific polymorphism to interspecific divergence: genetics of
438 pigmentation in *Drosophila*. *Science* 326, 540–544. doi:10.1126/science.1176980.
439 Wright, T. R. F. (1987). "The genetics of biogenic amine metabolism, sclerotization, and
440 melanization in *Drosophila melanogaster*," in *Advances in Genetics* (Academic Press, Inc),
441 127–222. doi:10.1016/S0065-2660(08)60008-5.
442 Yassin, A., Bastide, H., Chung, H., Veuille, M., David, J. R., and Pool, J. E. (2016). Ancient
443 balancing selection at *tan* underlies female colour dimorphism in *Drosophila erecta*. *Nat.*
444 *Commun.* 7, 10400. doi:10.1038/ncomms10400.
445 Yassine, H., Kamareddine, L., and Osta, M. A. (2012). The Mosquito Melanization Response Is
446 Implicated in Defense against the Entomopathogenic Fungus Beauveria bassiana. *PLoS*
447 *Pathog.* 8, e1003029. doi:10.1371/journal.ppat.1003029.
448 Zhang, L., Martin, A., Perry, M. W., van der Burg, K. R. L., Matsuoka, Y., Monteiro, A., et al.
449 (2017a). Genetic basis of melanin pigmentation in butterfly wings. *Genetics* 205, 1537–
450 1550. doi:10.1534/genetics.116.196451.
451 Zhang, L., Mazo-Vargas, A., and Reed, R. D. (2017b). Single master regulatory gene coordinates
452 the evolution and development of butterfly color and iridescence. *Proc. Natl. Acad. Sci.*
453 *USA* 114, 10707–10712. doi:10.1073/pnas.1709058114.
454 Zhang, L., and Reed, R. D. (2017). "A practical guide to CRISPR/Cas9 genome editing in

Lepidoptera," in *Diversity and Evolution of Butterfly Wing Patterns*, eds. T. Sekimura and H. F. Nijhout (Singapore: Springer Singapore), 155–172. doi:10.1007/978-981-10-4956-9_8.

459 **Table 1: Molecular evolution of melanin pathway genes in Lepidoptera.** A summary of tests
460 of selection at the levels of individual sites, genes and branches. All the genes studied contained a
461 single conserved domain, except for two domains in *ebony*.
462

Gene	***aaNAT***	***black***	***DDC***	***ebony***	***pale***	***tan***
Number of species	37	44	41	39	38	36
Sequence length in nucleotides	852	1545	1503	2622	1689	1277
Percentage of sites with pervasive purifying selection	79.9	89.1	88.02	88.1	88.45	86.06
Percentage of sites with pervasive diversifying selection	0	0	0	0	0	0
Number of branches under episodic diversifying selection	0	2	0	11	2	3
Evidence for gene-wide episodic diversifying selection	Yes	Yes	No	Yes	Yes	No
Number of sites under episodic selection	1	0	0	2	2	3
Global omega value for the gene	0.09	0.06	0.04	0.08	0.04	0.08
Omega value for conserved domain 1	0.07	0.05	0.03	0.07	0.02	0.07
Omega value for conserved domain 2	-	-	-	0.05	-	-

463

Figure 1: Melanin pathway genes and their phenotypic effects in Lepidoptera. The proposed melanin pathway (Wright, 1987; Zhang et al., 2017) illustrates the genes/enzymes (colored in purple) that catalyze different steps in the production of four major pigments. The end products of the pathway conjugate with sclerotin to produce differently colored scales (Vavricka et al., 2010), as illustrated. Each gene also regulates individual wing elements in different species of butterflies (green arrows), as deciphered from their knockout phenotypes (summarized in Table S1).

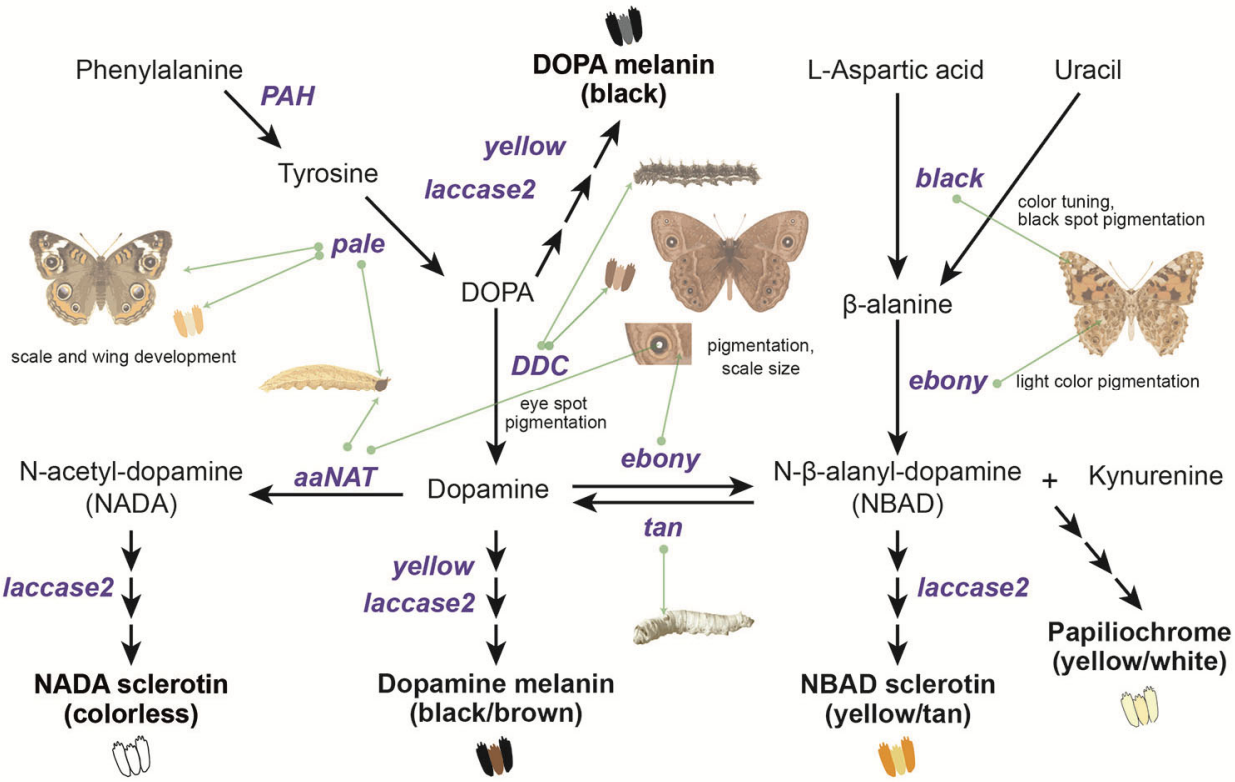

Figure 2: Molecular evolution of selected genes in the melanin pathway. Molecular evolution is shown with individual rates of synonymous (blue) and nonsynonymous substitutions (orange) for each codon (top panels) and dN/dS ratios for individual codons (lower panels). Functional domains for each gene are highlighted along with sites under episodic diversifying selection (green arrows). Rates of substitutions are compared between genes in the boxplot (right) where dN values significantly differ across genes (p<0.001, see Table S3). Groups that do not differ statistically are represented by the same letter.

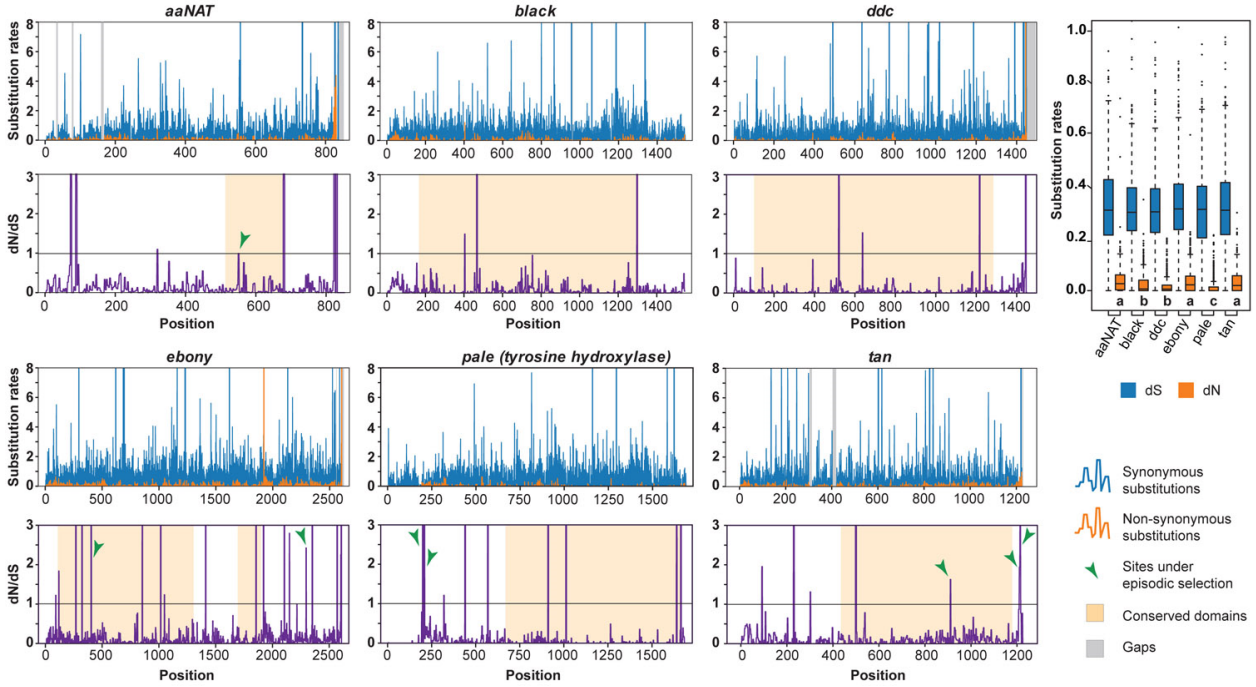

Figure 3: Expression of the six melanin pathway genes across developmental stages of *Papilio polytes*. Normalized counts obtained from transcriptome data are plotted for each stage, tissue and sex (beyond 5th instar larvae). The developmental stages are color-coded and pictorially represented at the bottom.

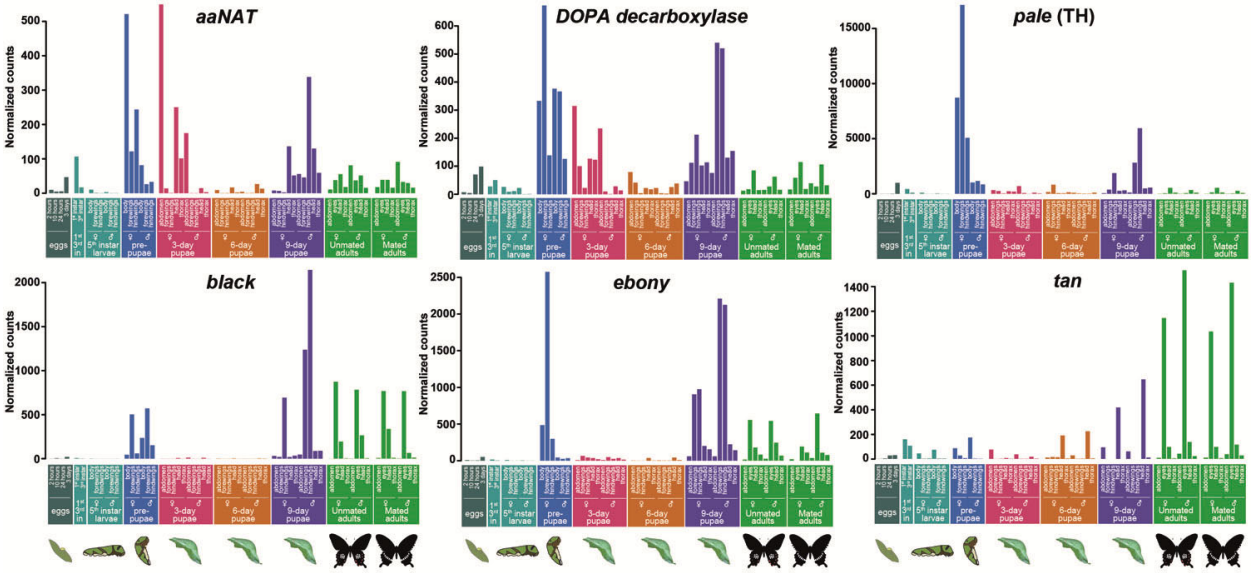

SUPPLEMENTARY MATERIAL

Table S1: Functional roles of melanin pathway genes selected for this study.

Gene	Organism	Function	Phenotype governed	Experiments	Citation
pale (tyrosine hydroxylase)	*B. anynana*	catalyzes Tyrosine to DOPA conversion	larval head capsule pigmentation; scale development, pigmentation and structural rigidity	CRISPR/cas9	(Matsuoka and Monteiro, 2018)
	J. coenia	catalyzes Tyrosine to DOPA conversion	cuticle development; expansion of wings; scale development	CRISPR/cas9	(Zhang et al., 2017a)
DOPA-decarboxylase (DDC)	*B. anynana*	conversion of DOPA to dopamine	scale hardening in colored scales; arrangement of cross ribs on color scales	CRISPR/cas9	(Matsuoka and Monteiro, 2018)
	V. cardui	conversion of DOPA to dopamine	melanization and sclerotization of larval mouth parts	CRISPR/cas9	(Zhang et al., 2017a)
ebony	*B. anynana*	converts dopa-melanin to NBAD, required for NBAD-sclerotin	repressor of melanin synthesis; responsible for lighter pigmentation such as, gold and beige; affects scale size	CRISPR/cas9	(Matsuoka and Monteiro, 2018)
	V. cardui *B. anynana* *J. coenia*		light pigmentation and coloration of eyespots; marginal band and central bands	CRISPR/cas9	(Zhang et al., 2017a)
black	*V. cardui*	conversion of aspartate to β-alanine (NBAD precursor)	knock out causes hypermelanism; local black activity may be essential for color-tuning some elements	CRISPR/cas9	(Zhang et al., 2017a)
tan	*B. mori*	conversion of NBAD to dopamine	required for normal black markings	expression studies	(Futahashi et al., 2010), (Zhang et al., 2017a)
arylalkylamine N-acetyltransferase (aaNAT)	*B. anynana*	converts dopamine to NADA, results in colorless sclerotin	brown head capsule pigmentation in late larvae; essential for white eyespot centers	CRISPR/cas9	(Matsuoka and Monteiro, 2018)

Table S2: Genomes used in this study. The accession codes of 53 Lepidopteran genomes and Dipteran outgroups along with details of extracted genes for each comparison are summarized in Excel file TableS2.SpeciesListAndGenomeDetails.xlsx.

Table S3: *p*-values for pair-wise comparisons of nonsynonymous substitution rates shown in Fig. 2. Significance of p<0.001 is indicated with ***.

Gene comparisons for dS	Z statistic	p (unadjusted)	p (adjusted)	Significance
aanat-black	1.66110505	0.09669235	1	-
aanat-ddc	1.43518131	0.15123544	1	-
black-ddc	-0.2631673	0.79242163	1	-
aanat-ebony	0.68234543	0.49502055	1	-
black-ebony	-1.41176586	0.15801891	1	-
ddc-ebony	-1.10020745	0.27124175	1	-
aanat-pale	1.45306465	0.14620581	1	-
black-pale	-0.28465403	0.77590921	1	-
ddc-pale	-0.01331159	0.9893792	1	-
ebony-pale	1.12743228	0.25955976	1	-
aanat-tan	0.66414217	0.50659932	1	-
black-tan	-1.10445915	0.26939402	1	-
ddc-tan	-0.84928716	0.39572152	1	-
ebony-tan	0.07772577	0.9380462	1	-
pale-tan	-0.85922025	0.39021901	1	-

Gene comparisons for dN	Z statistic	p (unadjusted)	p (adjusted)	Significance
aanat-black	5.899968	3.64E-09	5.45E-08	***
aanat-ddc	6.949501	3.67E-12	5.50E-11	***
black-ddc	1.334072	1.82E-01	1.00E+00	-
aanat-ebony	1.229317	2.19E-01	1.00E+00	-
black-ebony	-6.543908	5.99E-11	8.99E-10	***
ddc-ebony	-7.9514	1.84E-15	2.77E-14	***
aanat-pale	10.917824	9.47E-28	1.42E-26	***
black-pale	6.113977	9.72E-10	1.46E-08	***
ddc-pale	4.689634	2.74E-06	4.11E-05	***
ebony-pale	13.590144	4.58E-42	6.87E-41	***
aanat-tan	2.027325	4.26E-02	6.39E-01	-
black-tan	-4.321267	1.55E-05	2.33E-04	***
ddc-tan	-5.528088	3.24E-08	4.86E-07	***
ebony-tan	1.239223	2.15E-01	1.00E+00	-
pale-tan	-10.077773	6.93E-24	1.04E-22	***

Figure S1: Phylogenetic reconstruction of the species tree and gene trees for the six melanin pathway genes. A. Genus level species tree for the taxa used in this study. **B-G**. Gene trees reconstructed using the sequences extracted from genomes of the respective taxa. Green and purple branches represent moths and butterflies, respectively, while gray branches denote outgroups.

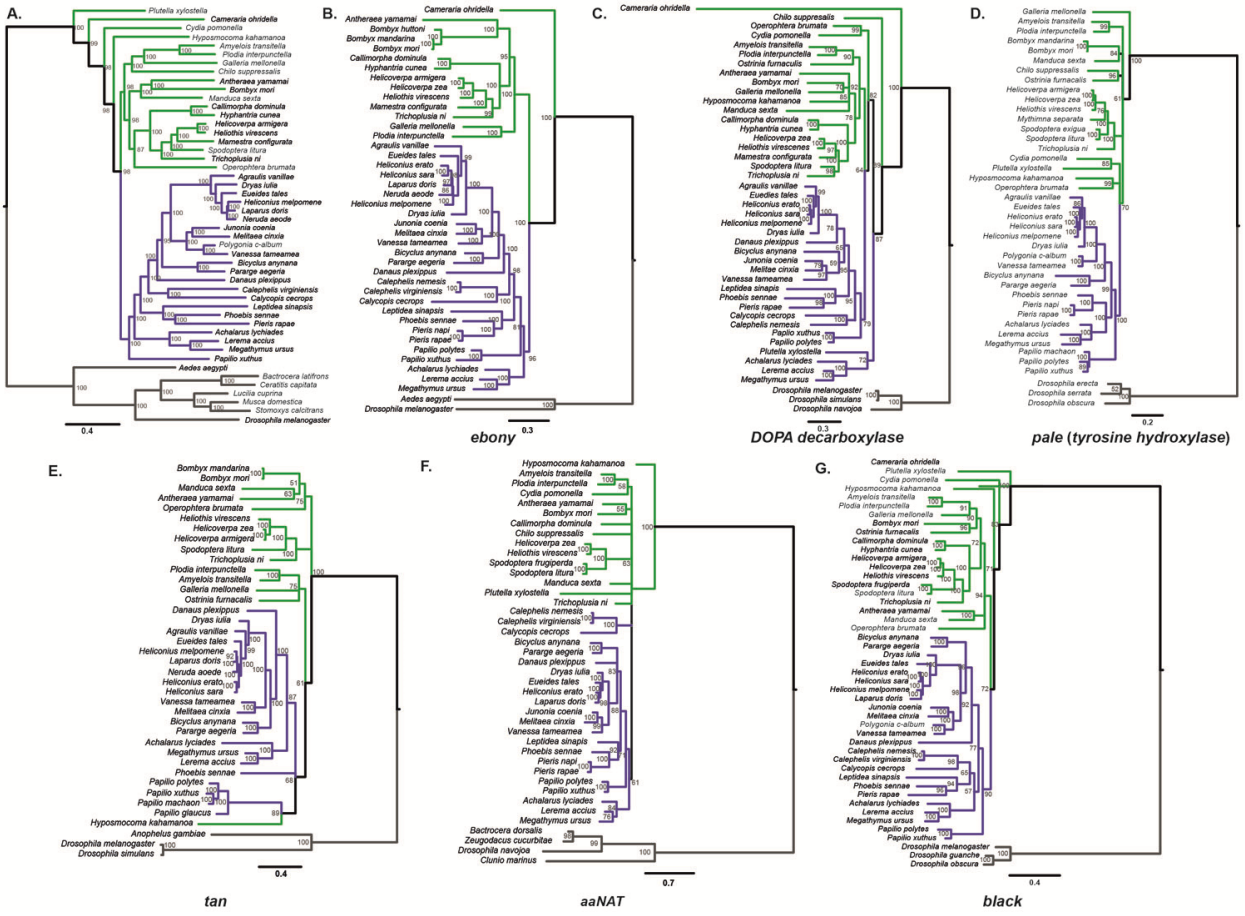

Figure S2: Developmental expression patterns of *aaNAT*, *DDC and pale* in log2 scale.